Psoralidin induces autophagy through ROS generation which inhibits the proliferation of human lung cancer A549 cells

Psoralidin (PSO), a natural furanocoumarin, is isolated from Psoralea corylifolia L. possessing anti-cancer properties. However, the mechanisms of its effects remain unclear. Herein, we investigated its anti-proliferative effect and potential approaches of action on human lung cancer A549 cells. Cell proliferation and death were measured by MTT and LDH assay respectively. Apoptosis was detected with Hoechst 33342 staining by fluorescence microscopy, Annexin V-FITC by cytometry and Western blot analysis for apoptosis-related proteins. The autophagy was evaluated using MDC staining, immunofluorescence assay and Western blot analyses for LC3-I and LC3-II. In addition, the reactive oxygen species (ROS) generation was measured by DCFH2-DA with flow cytometry. PSO dramatically decreased the cell viabilities in dose- and time- dependent manner. However, no significant change was observed between the control group and the PSO-treated groups in Hoechst 33342 and Annexin V-FITC staining. The expression of apoptosis-related proteins was not altered significantly as well. While the MDC-fluorescence intensity and the expression ratio of LC3-II/LC3-I was remarkably increased after PSO treatment. Autophagy inhibitor 3-MA blocked the production of LC3-II and reduced the cytotoxicity in response to PSO. Furthermore, PSO increased intracellular ROS level which was correlated to the elevation of LC3-II. ROS scavenger N-acetyl cysteine pretreatment not only decreased the ROS level, reduced the expression of LC3-II but also reversed PSO induced cytotoxicity. PSO inhibited the proliferation of A549 cells through autophagy but not apoptosis, which was mediated by inducing ROS production.

1 **Psoralidin induces autophagy through ROS generation which inhibits the proliferation of**

2 **human lung cancer A549 cells**

3 Wenhui Hao†, Xuenong Zhang†, Wenwen Zhao, Xiuping Chen*

4 State Key Laboratory of Quality Research in Chinese Medicine, Institute of Chinese Medical Sciences,

5 University of Macau, Macao, China

6 Running title: Psoralidin induces autophagy

7 *Send correspondence to: Dr. Xiuping Chen

8 Address: Institute of Chinese Medical Sciences, University of Macau, Av. Padre Tomas Pereira S.J.,

9 Taipa, Macau, China

10 xpchen@umac.mo

11 Tel: +853-88224679

12 †Co-first author.

13 **ABSTRACT**

14 Psoralidin (PSO), a natural furanocoumarin, is isolated from *Psoralea corylifolia L.* possessing

15 anti-cancer properties. However, the mechanisms of its effects remain unclear. Herein, we

16 investigated its anti-proliferative effect and potential approaches of action on human lung cancer

17 A549 cells. Cell proliferation and death were measured by MTT and LDH assay respectively.

18 Apoptosis was detected with Hoechst 33342 staining by fluorescence microscopy, Annexin V-

19 FITC by cytometry and Western blot analysis for apoptosis-related proteins. The autophagy was

20 evaluated using MDC staining, immunofluorescence assay and Western blot analyses for LC3-I

21 and LC3-II. In addition, the reactive oxygen species (ROS) generation was measured by $DCFH_2$-

22 DA with flow cytometry. PSO dramatically decreased the cell viabilities in dose- and time-

23 dependent manner. However, no significant change was observed between the control group and

24 the PSO-treated groups in Hoechst 33342 and Annexin V-FITC staining. The expression of

25 apoptosis-related proteins was not altered significantly as well. While the MDC-fluorescence

26 intensity and the expression ratio of LC3-II/LC3-I was remarkably increased after PSO treatment.

27 Autophagy inhibitor 3-MA blocked the production of LC3-II and reduced the cytotoxicity in

28 response to PSO. Furthermore, PSO increased intracellular ROS level which was correlated to the

29 elevation of LC3-II. ROS scavenger N-acetyl cysteine pretreatment not only decreased the ROS

30 level, reduced the expression of LC3-II but also reversed PSO induced cytotoxicity. PSO

31 inhibited the proliferation of A549 cells through autophagy but not apoptosis, which was

32 mediated by inducing ROS production.

33 **Keywords:** Psoralidin; ROS; Autophagy; Cancer

34 **INTRODUCTION**

35 *Psoralea corylifolia Leguminosae* (L.), an herb widely distributed in China and Southeastern

36 Asian countries, has been used as a multi-purpose medicinal plant (*Zhao et al., 2005*). The fully

37 mature dried fruit of this plant is well-known as traditional Chinese medicine called "Buguzhi",

38 and is used to treat a wide range of diseases. Previous screening studies have reported that some

39 extracts and active fractions of *P. corylifolia L.* exhibited cytotoxicity and inhibition of chemical

40   carcinogenesis (*Latha et al., 2000*; *Latha and Panikkar, 1999*; *Whelan and Ryan, 2003*). The

41   major chemical constituents in *P. corylifolia L.* include coumarins, flavonoids and meroterpene

42   phenols (*Song et al., 2013*). Psoralidin (PSO, Fig. 1A), with coumarin structure, is one of the

43   bioactive components. It is reported that PSO shows cytotoxic effects against some cultured

44   human cancer cell lines (*Bronikowska et al., 2012*; *Kumar et al., 2010*; *Mar et al., 2001*; *Pahari*

45   *and Rohr, 2009*; *Yang et al., 1996*). In prostate cancer and HeLa cells, PSO enhanced TRAIL-

46   mediated apoptosis (*Bronikowska et al., 2012*; *Szliszka et al., 2011*). PSO induced apoptosis in

47   breast cancer cells by inhibiting NOTCH1 signaling (*Suman et al., 2013*). It also inhibits TNF-

48   mediated survival signaling in androgen independent prostate cancer cells (*Srinivasan et al.,*

49   *2010*). However, its effect on autophagy, a nonapoptotic form of programmed cell death, remains

50   to be clarified. Herein, we demonstrated that PSO is an anti-proliferative natural compound of on

51   human lung cancer A549 cells. It induces autophagy rather than apoptosis, which was triggered

52   by increasing intracellular ROS generation.

53   **MATERIALS AND METHODS**

54   **Reagents and cell culture**

55   Psoralidin (>98%) was purchased from Chengdu Preferred Biotech Co. Ltd (Chengdu,China).

56   Dimethyl sulfoxide (DMSO), MTT, Hoechst 33342, monodansylcadaverine (MDC), propidium

57   iodide (PI), 3-methyladenine (3-MA), Ac-DEVD-CHO, z-VAD-FMK, DAPI, CM-H$_2$DCF-DA,

58   N-acetyl cysteine (NAC), Annexin V-FITC were from Sigma Aldrich (St. Louis, MO, USA).

59   Cytotoxicity Detection Kit (lactate dehydrogenase, LDH) was obtained from Roche Diagnostics

60   (Mannheim, Germany). Antibodies against LC3, Bcl-2, BAX, PARP, Caspase-3, Caspase-9 and

61   GAPDH were purchased from Cell Signaling Technology (Beverly, MA, USA).

62   The human lung cancer cell line A549, obtained from American Type Culture Collection

63   (ATCC, USA), was cultured in RPMI 1640 (Gibco) supplemented with 10% (v/v) fetal bovine

64 serum at 37°C in a humidified atmosphere of 5% CO_2.

MTT assay and LDH assay

66 Cells in the exponential growth phase were seeded in 96-well culture plates (5000 cells per well),

67 treated with various concentrations (1.25, 2.5, 5, 10, 20, 30 and 40 µM) of PSO for indicated

68 time. After incubation, 20 µl MTT solutions (5 mg/ml) was added to each well and incubated for

69 further 4 h. Then the supernatant was removed and the resulting crystals were dissolved in

70 DMSO. The absorbance of each well was measured using a microplate reader (PerkinElmer,

71 USA) at 570 nm. The cell viability was calculated by the formula: cell viability (%) = (average

72 absorbance of treated groups/average absorbance of control group) × 100%. A commercial

73 cytotoxicity detection kit was used to evaluate the LDH release from cells after treatment with

74 different concentrations of PSO according to the manufacturer's protocol.

Cell cycle analysis

76 After treated with PSO, cells were harvested and washed with cold phosphate buffer saline

77 (PBS), and were fixed with 70% ethanol overnight at -20°C. The fixed cells were then washed

78 twice with cold PBS, and the supernatant was removed. Cells were stained with PI staining

79 solution (10 µg/ml RNase A and 50 µg/ml PI) at 37°C for 30 min in dark. The cell cycle

80 distribution was analyzed using a flow cytometry provided with the Cell-Quest software (Becton

81 Dickinson, USA).

Apoptosis detection

83 Hoechst 33342 staining and Annexin V-FITC staining were performed to detect apoptosis. For

84 Hoechst 33342 staining, A549 cells were washed with PBS and stained with Hoechst 33342 (1

85 µg/ml in PBS) at room temperature for 20 min, the fluorescence was observed by a fluorescence

86 inverted microscopy. For Annexin V-FITC staining, the treated cells were collected, washed and

87 then stained with Annexin V-FITC at room temperature for 15 min, the percentage of apoptotic

88 cells were analyzed by flow cytometry.

89 **MDC staining and immunofluorescence**

90 The autophagic activity was evaluated using MDC staining and immunofluorescence for LC3-II

91 by fluorescence microscopy as described previously (*Zhang et al., 2013*). In brief, the treated

92 cells were incubated with 0.05 mM MDC for 15 min in the dark, then washed with PBS twice

93 and immediately analyzed by a fluorescence inverted microscopy. For immunofluorescence, the

94 treated cells were fixed with 4% paraformaldehyde and blocked with 2% BSA for 30 min,

95 incubated with primary antibody against LC3-II at 4°C overnight, then washed with PBS twice

96 and incubated with fluo-conjugated secondary antibody at room temperature for another 1 h. The

97 nuclei were stained with DAPI and the stained cells were observed under a fluorescence inverted

98 microscope using filter set for FITC and DAPI.

99 **Western blot analysis**

100 After treated with PSO, cells were washed with cold PBS and lysed with RIPA lysis buffer (Santa

101 Cruz, USA) to extract the total proteins. The concentrations of the total proteins were determined

102 by Pierce BCA protein assay kit (Thermo Scientific, USA). Equivalent amounts of total proteins

103 from each sample were separated by SDS-PAGE, and then transferred onto a PVDF membrane.

104 After blocking with PBS containing 0.1% Tween-20 and 5% nonfat milk for 1 h, the transferred

105 membrane was incubated with a specific primary antibody at 4°C overnight, followed by

106 incubation with the corresponding secondary antibody. Washing the membrane and specific

107 protein bands were visualized using an ECL Advanced Western Blot detection Kit, the

108 densitometric analysis of bands was performed using the Quantity-One Software.

109 **Determination intracellular ROS production**

110 Intracellular ROS production was measured by flow cytometry analysis using CM-H$_2$DCF-DA as

111 fluorescence probe. After PSO treatment, cells were washed and incubated with DCFH$_2$-DA

112 (5μM) for 30 min at 37°C in the dark. The stained cells were analyzed by flow cytometry.

113 **Statistical analysis**

114 Data are expressed as the means ± SD from at least three independent experiments. The

115 differences between groups were analyzed by one-way ANOVA with Tukey's posthoc tests,

116 significance of difference was indicated as $*P < 0.05$ or $**P < 0.01$.

117 **RESULTS**

118 **The cytotoxicity of PSO in A549 cells**

119 The effects of PSO in A549 cells were detected using MTT assay. As shown in Fig. 1B, the

120 inhibition of PSO in A549 cell proliferation was exhibited both in time- and concentration-

121 dependent manners. The calculated IC_{50} after 24, 48 and 72 h treatment were 19.2, 15.4 and 11.8

122 µM respectively. Furthermore, after treatment with varies concentrations of PSO for 24 h, the

123 LDH release from A549 cells was increased in a concentration-dependent manner (Fig. 1C).

124 **PSO induced cell cycle arrest at G1 phase**

125 To measure the underlying mechanism responsible for the anti-proliferation effect of PSO in

126 A549 cells, cell cycle distribution was detected by flow cytometry analysis of DNA content using

127 PI staining. As shown in Fig. 2, PSO in concentrations of 10 and 20 µM induced an increase in

128 the percentage of cells in G1 phase. Compared with the control group, 20 µM PSO treatment

129 groups showed significant increase ($P < 0.05$) in the proportion of G1 phase cells (Fig. 2B).

130 **PSO showed little effect on apoptosis in A549 cells**

131 Hoechst 33342 staining and flow cytometry assay using Annexin V-FITC staining were

132 performed to determine whether apoptosis was induced by PSO. As shown in Fig. 3A, both the

133 untreated and treated cells had regular and round-shaped nuclei and the characteristic

134 morphological changes of apoptosis were not observed. Flow cytometry analysis using Annexin

135 V-FITC staining showed that treatment A549 cells with different concentrations of PSO did not

136 alter the percentage of Annexin V-FITC positive cells compared with control group (Fig. 3B).

137 Furthermore, the expressions of some apoptosis-related proteins were analyzed by Western blot.

138 After the treatment with PSO for 24 h, the expression of apoptosis-related proteins Bcl-2, BAX,

139 Caspase-3, Caspase-9 and PARP did not alter significantly (Fig. 3C). These results suggest that

140 PSO maybe not induce apoptosis in A549 cells.

141 In addition, the pancaspase inhibitor Z-VAD-FMK and caspse-3 inhibitor AC-DEVD-CHO

142 were used to confirm the effect of PSO in A549 cells. As shown in Fig. 3D, Z-VAD-FMK and

143 AC-DEVD-CHO failed to protect A549 cells from death caused by PSO. These results

144 collectively indicate that the cell death induced by PSO is in a caspase-independent non-apoptotic

145 manner.

146 PSO induced autophagic cell death in A549 cells

147 To test the autophagic activity induced by PSO, MDC staining was performed firstly. As shown

148 in Fig. 4A, the control cells showed faint fluorescence, while cells treated with PSO accumulated

149 MDC into granular structures of high fluorescence intensity. The immunofluorescence for LC3-II

150 was executed to further examine the formation of autophagic vesicles. Compared with the

151 untreated cells, A549 cells treated with PSO exhibited increases in both the number and size of

152 LC3-II-postive puncta (Fig. 4B). Western blot analysis for LC3 showed a remarkable increase of

153 LC3-II in response to PSO treatment both in concentration- and time-dependent manner (Fig. 4C

154 and D). Furthermore, this increase of LC3-II could be blocked in the presence of autophagy

155 inhibitor 3-MA (Fig. 4E). In addition, pretreatment with 3-MA significantly prevented cell death

156 induced by PSO (Fig. 4 F). Taken together, these results suggest that PSO induces autophagic cell

157 death instead of apoptosis in A549 cells.

158 PSO induced ROS generation and NAC reversed PSO-induced autophagy and cell death

159 As shown in Fig. 5A and B, PSO induced ROS generation in a concentration-dependent manner

160 in A549 cells. NAC pretreatment efficiently attenuated PSO induced elevation of ROS levels.

161 Meanwhile, pretreatment with NAC prevented the increase of LC3-II and cell death in response

162 to PSO (Fig. 5C and D). These results suggested that the production of ROS plays a key role in

163 the PSO-induced autophagy and subsequent cell death.

DISCUSSION

164

165 PSO is natural product isolated from *Psoralea corylifolia L.*, which is an important medical herb

166 prescribed in traditional Chinese medicine. Previous reports demonstrated that PSO showed

167 significant antibacterial (*Khatune et al., 2004*), antidepressant-like properties (*Yi et al., 2008*),

168 antioxidant (*Xiao et al., 2010*) activities. It also showed inhibitory effect on protein tyrosine

169 phosphatase 1B *in vitro* (*Kim et al., 2005*), induction of quinone reductase activity (*Lee et al.,*

170 *2009*), and inhibitory effect on LPS-induced iNOS expression (*Chiou et al., 2011*). Furthermore, it

171 was found that PSO could act as an ER agonist (*Liu et al., 2014*) and was a dual inhibitor of

172 COX-2 and 5-LOX (*Yang et al., 2011*). Herein, the anti-proliferative effect of PSO was

173 investigated.

174 Previous studies showed that PSO inhibited the proliferation of SNU-1 and SNU-16 gastric

175 carcinoma cell lines (*Yang et al., 1996*), HT-29 colon and MCF-7 breast human cancer cell lines

176 (*Mar et al., 2001*). In present study, we showed that PSO inhibited proliferation on human lung

177 cancer A549 cells with IC_{50} at the range of 10 to 20 μM, which suggested PSO possesses a

178 potential cytotoxicity to cancer cells. This was further confirmed by PSO induced LDH release in

179 the culture medium. The effect of PSO on cell showed that PSO induced an increase in the

180 percentage of cells in G1 phase, suggesting PSO could cause the cell cycle arrest.

181 Apoptosis, a physiological process of programmed cell death, is one of the major types of

182 cell death caused by most chemotherapeutics. It has been reported that PSO enhanced TRAIL-

183 induced apoptosis in HeLa cells (*Bronikowska et al., 2012*) and prostate cancer cells (*Szliszka et*

184 *al., 2011*). In present study, the effect of PSO on apoptosis in A549 cells was detected using

185 Hoechst 33342 staining by fluorescence microscopy and Annexin V-FITC staining by flow

186 cytometry. In addition, the expressions of apoptosis-related proteins such as Bcl-2, Bax, Caspase-

187 3, Caspase-9 and PARP were examined by Western blot. There was no significant nuclear

188 changes in Hoechst 33342 staining were observed. Furthermore, no significant differences in the

189 percentage of Annexin V-FITC positive cells and apoptosis-related proteins expression between

190 the control groups and PSO treated groups. In addition, the pancaspase inhibitor Z-VAD-FMK

191 and caspse-3 inhibitor AC-DEVD-CHO failed to protect A549 cells from PSO induced death.

192 Taken together, these results indicated that apoptosis might play a minor role in PSO induce cell

193 death in A549 cells.

194   Autophagy, a cellular process responsible for the degradation of cytoplasmic components

195 through an autophagosomal-lysosomal pathway, has been implicated to play a key role in cancer

196 initiation and progress (*Janku et al., 2011*). A panel of natural products has been identified to

197 induce both apoptotic and autophagic cell death. PSO showed cytotoxicity to A549 cells but did

198 not induce apoptosis. Therefore, we detected whether PSO induced autophagic cell death in A549

199 cells. MDC is an acidotropic dye that labels late stage autophagosomes or autophagic vesicles.

200 During autophagosome formation, LC3-I is incorporated into autophagosome membranes

201 mediated by Atg3 and Atg7, which results in the conversion of cytosolic LC3-I into membrane-

202 bound form LC3-II (*Tanida et al., 2004*). Thus, the both the MDC staining and the expression

203 ratio of LC3-I to LC3-II provides simple indicators for autophagy activity and has been widely

204 used to monitor the autophagic activities (*Klionsky et al., 2012*). Present results showed that PSO

205 induced MDC staining, punctate staining dots for LC3-II□and increased protein expression ratio

206 of LC3-II/LC3-I suggesting that PSO caused autophagy in A549 cells. Furthermore, pretreatment

207 with 3-MA, an autophagy inhibitor, reversed PSO induced significantly protein expression ratio

208 of LC3-II/LC3-I and cell death induced by PSO. Taken together, these results suggested that PSO

209 induced autophagic cell death instead of apoptosis in A549 cells. To the best of our knowledge,

210 this is first report on the effect of PSO on autophagy.

211   Accumulated evidence suggested that ROS, a class of important multifaceted signaling

212 molecules implicated in a variety of cellular programs including autophagy (*Azad et al., 2009;*

213 *Dewaele et al., 2010; Scherz-Shouval and Elazar, 2011*). Though PSO showed anti-oxidant

214 activities in scavenging DPPH and ABTS free radicals in *ex vivo* models (*Wang et al., 2013; Xiao*

215 *et al., 2010*), it greatly induced ROS generation that resulted in the growth inhibition and promote

216 epithelial-mesenchymal transition in prostate cancer cells (*Das et al., 2013*). We also found that

217 PSO significantly induced DCF fluorescence in A549 cells suggesting the increase of

218 intracellular ROS generation. NAC, a ROS scavenger, pretreatment could significantly reverse

219 PSO induced autophagic biomarkers and cell death suggested that ROS mediated PSO-induced

220 autophagy and subsequent cell death.

221   In summary, as shown in Fig 6, our results show that PSO is a potential cytotoxic natural

222 compound. Instead of apoptosis, it induces ROS-triggered autophagy which inhibits the growth

223 of human lung cancer A549 cells.

Conflicts of interest

225 We declare that none of the authors has any conflict of interest related to the present work.

REFERENCE

227 **Azad MB, Chen Y, Gibson SB, 2009.** Regulation of autophagy by reactive oxygen species (ROS): implications for
228 cancer progression and treatment. *Antioxidants & redox signaling* **11**, 777-790.
229 **Bronikowska J, Szliszka E, Jaworska D, Czuba ZP, Krol W, 2012.** The coumarin psoralidin enhances anticancer
230 effect of tumor necrosis factor-related apoptosis-inducing ligand (TRAIL). *Molecules* **17**, 6449-6464.
231 **Chiou WF, Don MJ, Liao JF, Wei BL, 2011.** Psoralidin inhibits LPS-induced iNOS expression via repressing Syk-
232 mediated activation of PI3K-IKK-IkappaB signaling pathways. *Eur J Pharmacol* **650**, 102-109.
233 **Das TP, Suman S, Damodaran C, 2013.** Reactive oxygen species generation inhibits epithelial-mesenchymal
234 transition and promotes growth arrest in prostate cancer cells. *Molecular carcinogenesis*.
235 **Dewaele M, Maes H, Agostinis P, 2010.** ROS-mediated mechanisms of autophagy stimulation and their relevance in
236 cancer therapy. *Autophagy* **6**, 838-854.
237 **Janku F, McConkey DJ, Hong DS, Kurzrock R, 2011.** Autophagy as a target for anticancer therapy. *Nature
238 reviews. Clinical oncology* **8**, 528-539.
239 **Khatune NA, Islam ME, Haque ME, Khondkar P, Rahman MM, 2004.** Antibacterial compounds from the seeds
240 of Psoralea corylifolia. *Fitoterapia* **75**, 228-230.
241 **Kim YC, Oh H, Kim BS, Kang TH, Ko EK, Han YM, Kim BY, Ahn JS, 2005.** In vitro protein tyrosine
242 phosphatase 1B inhibitory phenols from the seeds of Psoralea corylifolia. *Planta Med* **71**, 87-89.
243 **Klionsky DJ, Abdalla FC, Abeliovich H, Abraham RT, Acevedo-Arozena A, Adeli K, Agholme L, Agnello M,
244 Agostinis P, Aguirre-Ghiso JA, et al., 2012.** Guidelines for the use and interpretation of assays for monitoring
245 autophagy. *Autophagy* **8**, 445-544.
246 **Kumar R, Srinivasan S, Pahari P, Rohr J, Damodaran C, 2010.** Activating stress-activated protein kinase-
247 mediated cell death and inhibiting epidermal growth factor receptor signaling: a promising therapeutic strategy for

248 prostate cancer. *Molecular cancer therapeutics* **9**, 2488-2496.
249 **Latha PG, Evans DA, Panikkar KR, Jayavardhanan KK, 2000.** Immunomodulatory and antitumour properties of
250 Psoralea corylifolia seeds. *Fitoterapia* **71**, 223-231.
251 **Latha PG, Panikkar KR, 1999.** Inhibition of chemical carcinogenesis by Psoralea corylifolia seeds. *Journal of*
252 *ethnopharmacology* **68**, 295-298.
253 **Lee SJ, Nam KW, Mar W, 2009.** Induction of quinone reductase activity by psoralidin isolated from Psoralea
254 corylifolia in mouse hepa 1c1c7 cells. *Arch Pharm Res* **32**, 1061-1065.
255 **Liu X, Nam JW, Song YS, Viswanath AN, Pae AN, Kil YS, Kim HD, Park JH, Seo EK, Chang M, 2014.**
256 Psoralidin, a coumestan analogue, as a novel potent estrogen receptor signaling molecule isolated from Psoralea
257 corylifolia. *Bioorganic & medicinal chemistry letters*.
258 **Mar W, Je KH, Seo EK, 2001.** Cytotoxic constituents of Psoralea corylifolia. *Arch Pharm Res* **24**, 211-213.
259 **Pahari P, Rohr J, 2009.** Total synthesis of psoralidin, an anticancer natural product. *The Journal of organic*
260 *chemistry* **74**, 2750-2754.
261 **Scherz-Shouval R, Elazar Z, 2011.** Regulation of autophagy by ROS: physiology and pathology. *Trends in*
262 *biochemical sciences* **36**, 30-38.
263 **Song P, Yang XZ, Yuan JQ, 2013.** Cytotoxic constituents from Psoralea corylifolia. *Journal of Asian natural*
264 *products research* **15**, 624-630.
265 **Srinivasan S, Kumar R, Koduru S, Chandramouli A, Damodaran C, 2010.** Inhibiting TNF-mediated signaling: a
266 novel therapeutic paradigm for androgen independent prostate cancer. *Apoptosis* **15**, 153-161.
267 **Suman S, Das TP, Damodaran C, 2013.** Silencing NOTCH signaling causes growth arrest in both breast cancer
268 stem cells and breast cancer cells. *British journal of cancer* **109**, 2587-2596.
269 **Szliszka E, Czuba ZP, Sedek L, Paradysz A, Krol W, 2011.** Enhanced TRAIL-mediated apoptosis in prostate
270 cancer cells by the bioactive compounds neobavaisoflavone and psoralidin isolated from Psoralea corylifolia.
271 *Pharmacol Rep* **63**, 139-148.
272 **Tanida I, Ueno T, Kominami E, 2004.** LC3 conjugation system in mammalian autophagy. *The international journal*
273 *of biochemistry & cell biology* **36**, 2503-2518.
274 **Wang TX, Yin ZH, Zhang W, Peng T, Kang WY, 2013.** [Chemical constituents from Psoralea corylifolia and their
275 antioxidant alpha-glucosidase inhibitory and antimicrobial activities]. *Zhongguo Zhong Yao Za Zhi* **38**, 2328-2333.
276 **Whelan LC, Ryan MF, 2003.** Ethanolic extracts of Euphorbia and other ethnobotanical species as inhibitors of
277 human tumour cell growth. *Phytomedicine : international journal of phytotherapy and phytopharmacology* **10**, 53-
278 58.
279 **Xiao G, Li G, Chen L, Zhang Z, Yin JJ, Wu T, Cheng Z, Wei X, Wang Z, 2010.** Isolation of antioxidants from
280 Psoralea corylifolia fruits using high-speed counter-current chromatography guided by thin layer chromatography-
281 antioxidant autographic assay. *Journal of chromatography. A* **1217**, 5470-5476.
282 **Yang HJ, Youn H, Seong KM, Yun YJ, Kim W, Kim YH, Lee JY, Kim CS, Jin YW, Youn B, 2011.** Psoralidin, a
283 dual inhibitor of COX-2 and 5-LOX, regulates ionizing radiation (IR)-induced pulmonary inflammation.
284 *Biochemical pharmacology* **82**, 524-534.
285 **Yang YM, Hyun JW, Sung MS, Chung HS, Kim BK, Paik WH, Kang SS, Park JG, 1996.** The cytotoxicity of
286 psoralidin from Psoralea corylifolia. *Planta Med* **62**, 353-354.
287 **Yi LT, Li YC, Pan Y, Li JM, Xu Q, Mo SF, Qiao CF, Jiang FX, Xu HX, Lu XB, et al., 2008.** Antidepressant-like
288 effects of psoralidin isolated from the seeds of Psoralea Corylifolia in the forced swimming test in mice. *Prog*
289 *Neuropsychopharmacol Biol Psychiatry* **32**, 510-519.
290 **Zhang X, Wei H, Liu Z, Yuan Q, Wei A, Shi D, Yang X, Ruan J, 2013.** A novel protoapigenone analog RY10-4
291 induces breast cancer MCF-7 cell death through autophagy via the Akt/mTOR pathway. *Toxicology and applied*
292 *pharmacology* **270**, 122-128.
293 **Zhao L, Huang C, Shan Z, Xiang B, Mei L, 2005.** Fingerprint analysis of Psoralea corylifolia L. by HPLC and LC-
294 MS. *Journal of chromatography. B, Analytical technologies in the biomedical and life sciences* **821**, 67-74.

295 **Figures and legends:**

296 **Fig. 1.** The cytotoxicity of psoralidin against human lung cancer A549 cells. (A) Chemical

297 structure of psoralidin. (B) Cells were treated with series concentrations of psoralidin for 24, 48,

298 or 72 h. The cell viability was measured by MTT assay, and the data were presented as means ±

299 SD from three independent experiments. (C) Cells were treated with 5, 10, 20 and 30 μM

300 psoralidin for 24 h, the LDH assay were performed. *$P < 0.05$ *vs*. Con and **$P < 0.01$ *vs*. Con.

301 Con, control

302 **Fig. 2.** Effect of psoralidin in cell cycle distribution of A549 cells. (A) Cells were treated with 5,

303 10 and 20 μM psoralidin for 24 h, and then stained with propidium iodide. The DNA content was

304 measured by flow cytometry. (B) The cell cycle distributions were analyzed and presented as

305 mean ± SD of three independent experiments. *$P < 0.05$ *vs*. Con. Con, control

306 **Fig. 3.** Psoralidin showed little effect on apoptosis in A549 cells. (A) Fluorescent staining of

307 nuclei in A549 cells by Hoechst 33342. (B) Flow cytometry assay to detect apoptosis in A549

308 cells using Annexin V staining. There is no significant difference among control group and

309 psoralidin treated groups. NS, no significant *vs*. Con. (C) The expression of apoptosis related

310 proteins were analyzed by Western blot in A549 cells receiving psoralidin treatment. (D) The cell

311 viability was measured by MTT assay after treatment with psoralidin in the absence or presence

312 of Z-VAD-FMK or Ac-DEVD-CHO. **$P < 0.01$ *vs*. Con; NS, no significant *vs*. psoralidin alone-

313 treated group. Con, control

314 **Fig. 4.** Psoralidin induced autophagic cell death in A549 cells. (A) Cells were stained with MDC

315   after psoralidin treatment. (B) Immunofluerescence analysis of endogenous LC3 in psoralidin-

316   treated A549 cells. (C) Cells were treated with indicated concentrations of psoralidin for 24 h.

317   The expression of LC3 was determined by Western blot. (D) Cells were treated with 20 μM

318   psoralidin for 6, 12, 24 or 48 h, expression of LC3 was determined by Western blot. (E) Cells

319   were treated with psoralidin, 3-MA or a combination of both, expression of LC3 was analyzed by

320   Western blot. (F) The cell viability was measured by MTT assay after treatment with psoralidin in

321   the absence or presence of 3-MA. **$P < 0.01$ *vs.* Con, # $P < 0.05$ *vs.* psoralidin alone-treated

322   group. Con, control

323   **Fig. 5.** Psoralidin induced ROS generation and NAC reversed psoralidin-induced autophagy and

324   cell death. (A) Cells were treated with indicated concentrations of psoralidin, and the intracellular

325   ROS generation was detected as described in Materials and methods. *$P < 0.05$ *vs.* Con and **P

326   < 0.01 *vs.* Con. (B) Cells were treated with 20 μM psoralidin in the absence or presence of NAC.

327   The intracellular ROS generation was detected, and data represent the means ± SD from three

328   independent experiments. **$P < 0.01$ *vs.* Con, #$P < 0.05$ *vs.* psoralidin alone-treated group. (C)

329   Cells were treated with 20 μM psoralidin in the absence or presence of NAC. The expression of

330   LC3 was analyzed by Western blot. (D) The cell viability was measured by MTT assay after

331   psoralidin with treatment in the absence or presence of NAC. **$P < 0.01$ *vs.* Con, #$P < 0.05$ *vs.*

332   psoralidin alone-treated group. Con, control

333   **Fig. 6.** Schematic diagram illustrates the underlying mechanism of psoralidin-induced cell death

334   in A549 cells.

Figure 1

Fig. 1. The cytotoxicity of psoralidin against human lung cancer A549 cells.

(A) Chemical structure of psoralidin. (B) Cells were treated with series concentrations of psoralidin for 24, 48, or 72 h. The cell viability was measured by MTT assay, and the data were presented as means ± SD from three independent experiments. (C) Cells were treated with 5, 10, 20 and 30 μM psoralidin for 24 h, the LDH assay were performed. *$P < 0.05$ *vs.* Con and **$P < 0.01$ *vs.* Con. Con, control <?xml:namespace prefix = o ns = "urn:schemas-microsoft-com:office:office" />
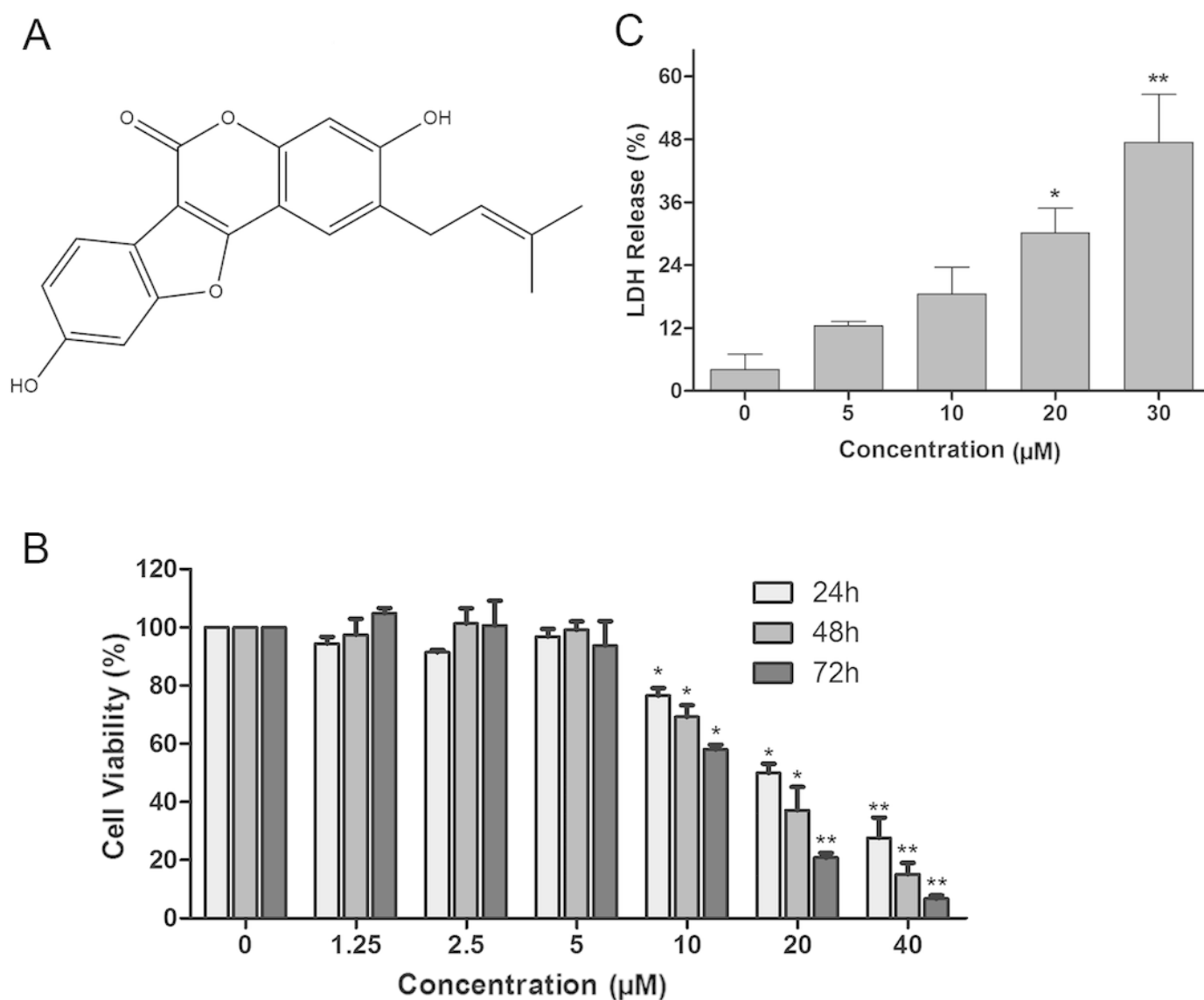
Figure 2

Fig. 2. Effect of psoralidin in cell cycle distribution of A549 cells.

(A) Cells were treated with 5, 10 and 20 µM psoralidin for 24 h, and then stained with propidium iodide. The DNA content was measured by flow cytometry. (B) The cell cycle distributions were analyzed and presented as mean ± SD of three independent experiments. *$P < 0.05$ *vs.* Con. Con, control‹?xml:namespace prefix = o ns = "urn:schemas-microsoft-com:office:office" />
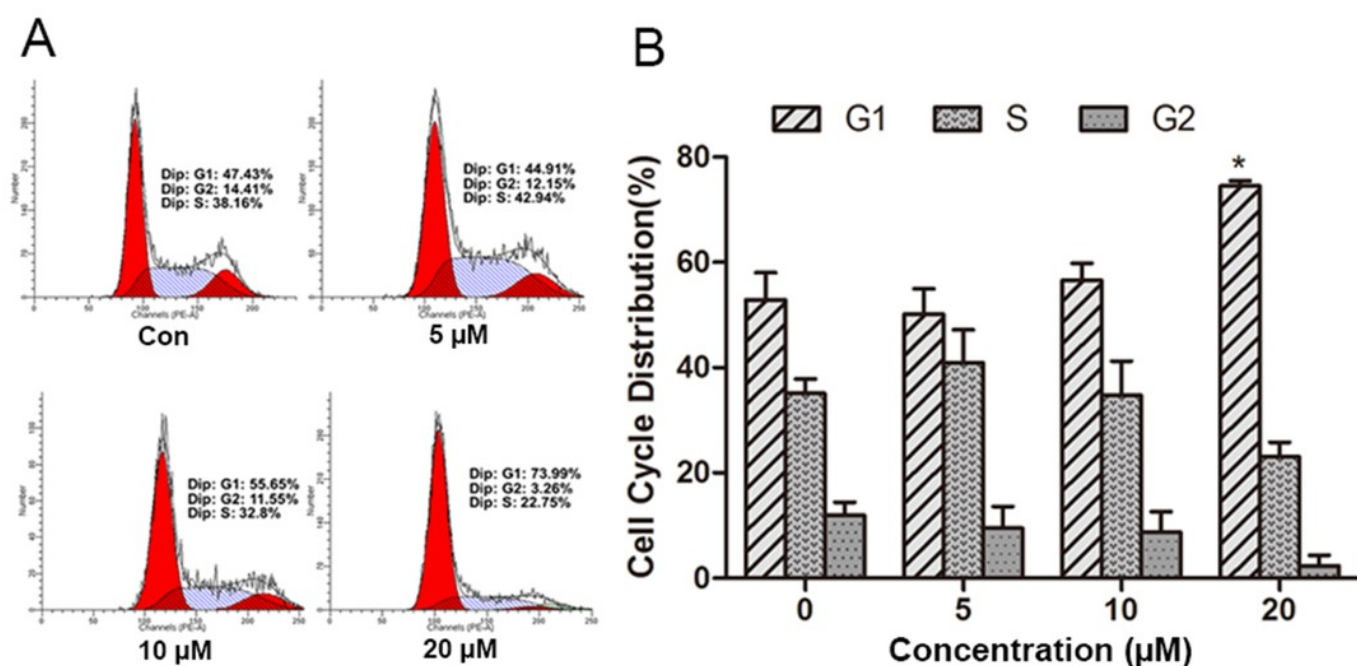
Figure 3

Fig. 3. Psoralidin showed little effect on apoptosis in A549 cells.

(A) Fluorescent staining of nuclei in A549 cells by Hoechst 33342. (B) Flow cytometry assay to detect apoptosis in A549 cells using Annexin V staining. There is no significant difference among control group and psoralidin treated groups. NS, no significant *vs.* Con. (C) The expression of apoptosis related proteins were analyzed by Western blot in A549 cells receiving psoralidin treatment. (D) The cell viability was measured by MTT assay after treatment with psoralidin in the absence or presence of Z-VAD-FMK or Ac-DEVD-CHO. **$P < 0.01$ *vs.* Con; NS, no significant *vs.* psoralidin alone-treated group. Con, control<?xml:namespace prefix = o ns = "urn:schemas-microsoft-com:office:office" />
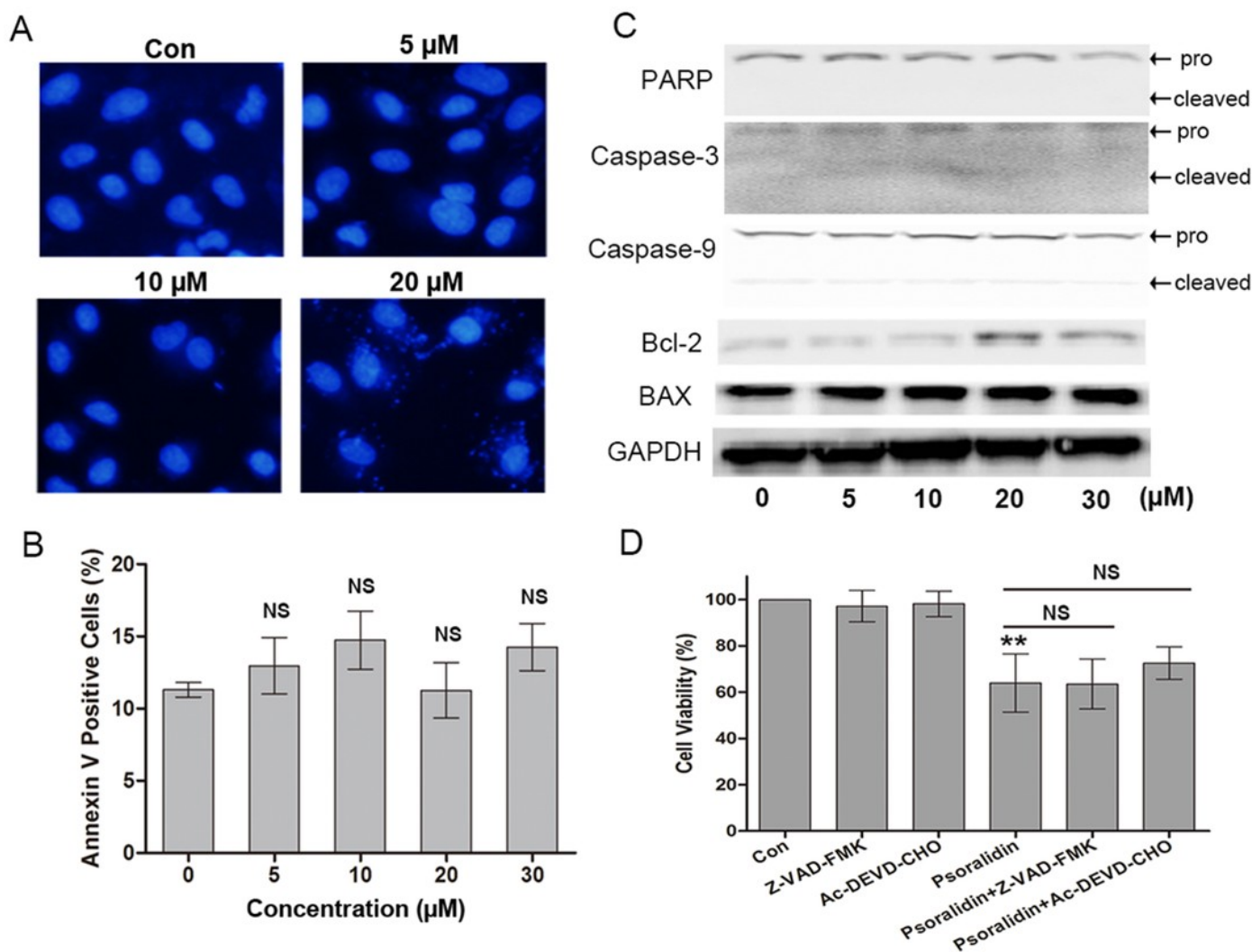
Figure 4

Fig. 4. Psoralidin induced autophagic cell death in A549 cells.

(A) Cells were stained with MDC after psoralidin treatment. (B) Immunofluerescence analysis of endogenous LC3 in psoralidin-treated A549 cells. (C) Cells were treated with indicated concentrations of psoralidin for 24 h. The expression of LC3 was determined by Western blot. (D) Cells were treated with 20 µM psoralidin for 6, 12, 24 or 48 h, expression of LC3 was determined by Western blot. (E) Cells were treated with psoralidin, 3-MA or a combination of both, expression of LC3 was analyzed by Western blot. (F) The cell viability was measured by MTT assay after treatment with psoralidin in the absence or presence of 3-MA. **$P < 0.01$ *vs.* Con, # $P < 0.05$ *vs.* psoralidin alone-treated group. Con, control<?xml:namespace prefix = o ns = "urn:schemas-microsoft-com:office:office" />
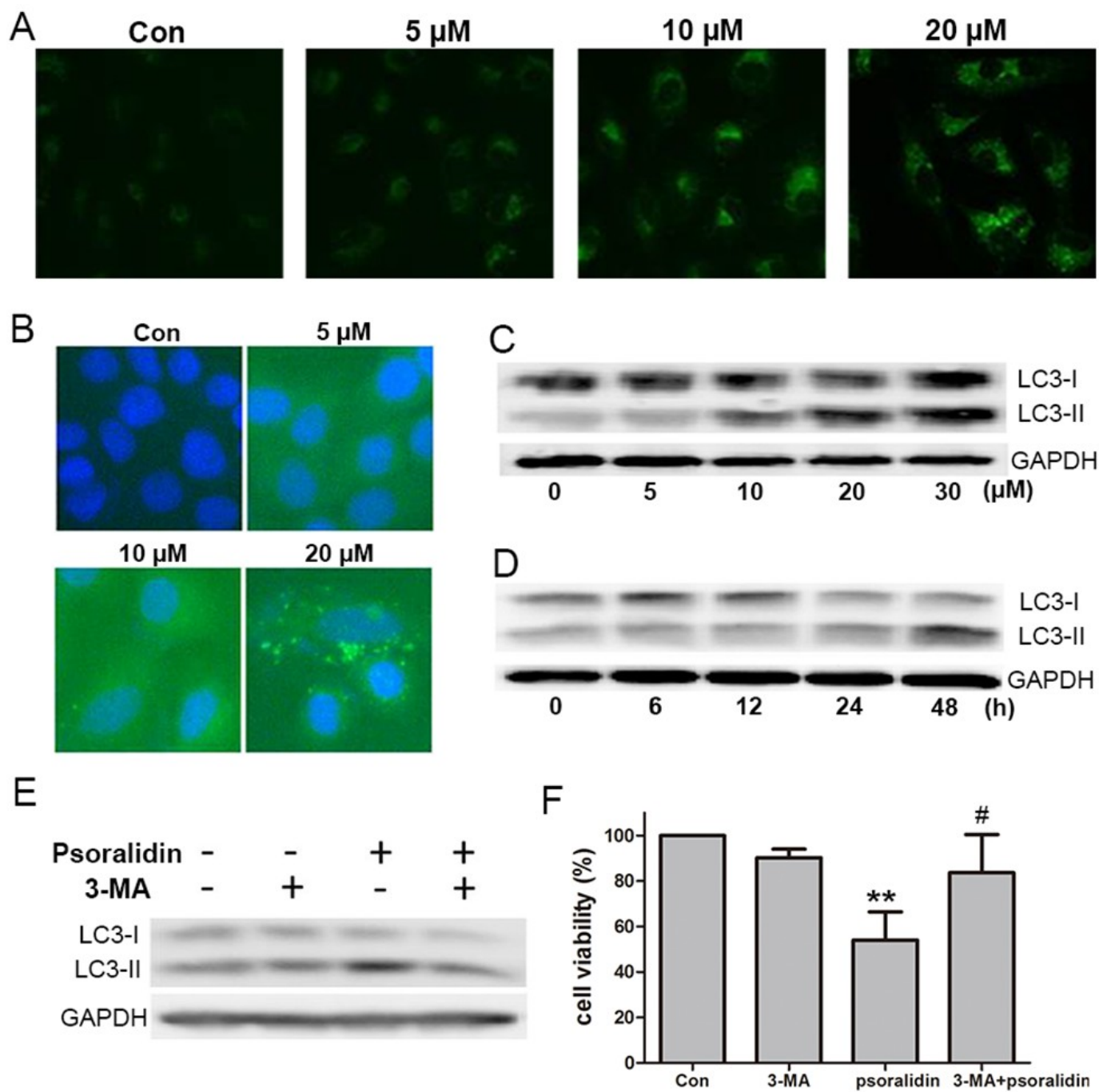
Figure 5

Fig. 5. Psoralidin induced ROS generation and NAC reversed psoralidin-induced autophagy and cell death.

(A) Cells were treated with indicated concentrations of psoralidin, and the intracellular ROS generation was detected as described in Materials and methods. *P < 0.05 *vs.* Con and **P < 0.01 *vs.* Con. (B) Cells were treated with 20 μM psoralidin in the absence or presence of NAC. The intracellular ROS generation was detected, and data represent the means ± SD from three independent experiments. ** P < 0.01 *vs.* Con, # P < 0.05 *vs.* psoralidin alone-treated group. (C) Cells were treated with 20 μM psoralidin in the absence or presence of NAC. The expression of LC3 was analyzed by Western blot. (D) The cell viability was measured by MTT assay after psoralidin with treatment in the absence or presence of NAC. ** P < 0.01 *vs.* Con, # P < 0.05 *vs.* psoralidin alone-treated group. Con, control<?xml:namespace prefix = o ns = "urn:schemas-microsoft-com:office:office" />
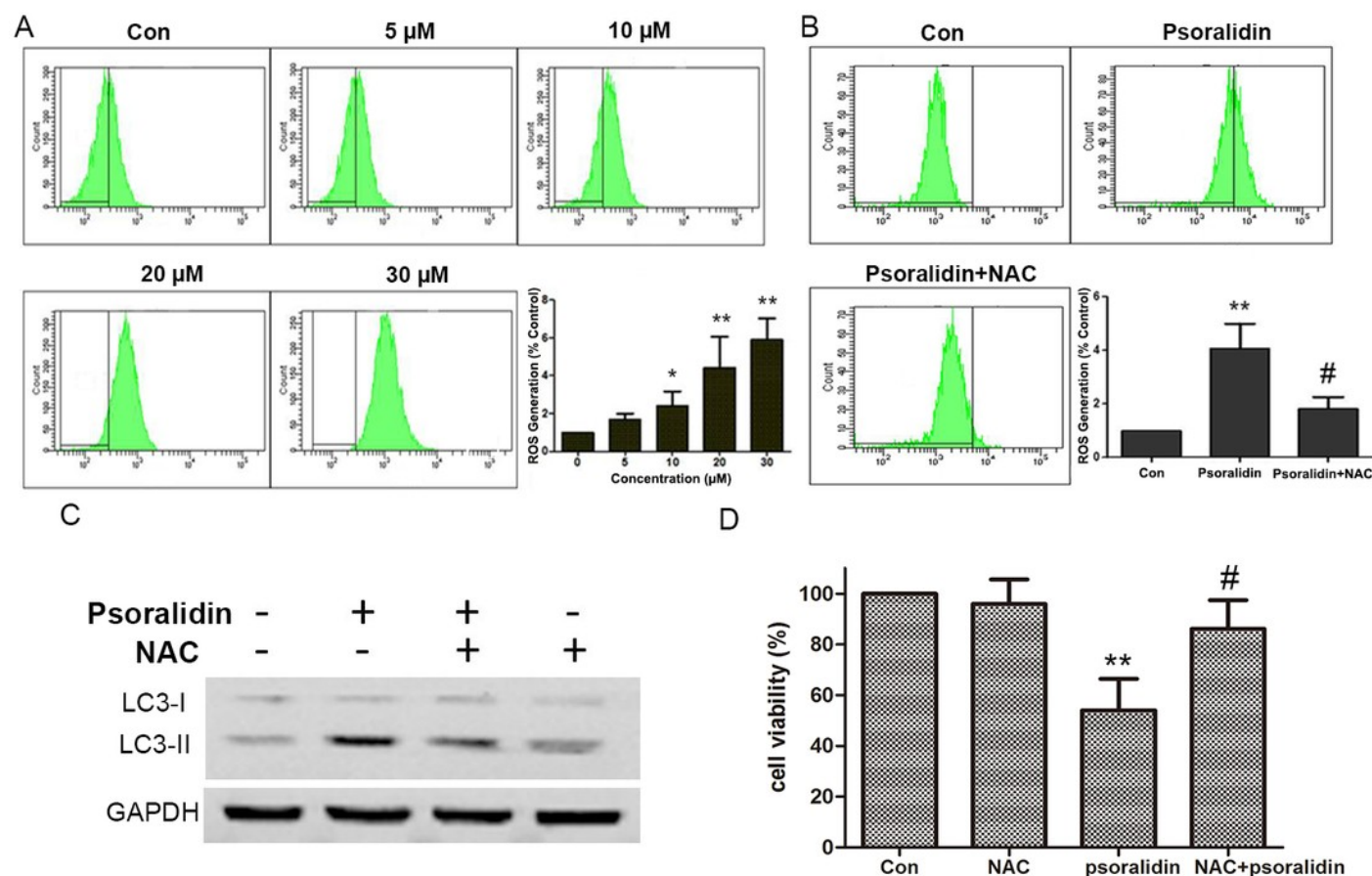
Figure 6

Fig. 6. Schematic diagram illustrates the underlying mechanism of psoralidin-induced cell death in A549 cells.<?xml:namespace prefix = o ns = "urn:schemas-microsoft-com:office:office" />